

## Mirage phenomena in superconducting quantum corrals

Markus Schmid, Arno P. Kampf

### Angaben zur Veröffentlichung / Publication details:

Schmid, Markus, and Arno P. Kampf. 2005. "Mirage phenomena in superconducting quantum corrals." *Annalen der Physik* 14 (9-10): 556-65.  
<https://doi.org/10.1002/andp.200510058>.

### Nutzungsbedingungen / Terms of use:

licgercopyright

Dieses Dokument wird unter folgenden Bedingungen zur Verfügung gestellt: / This document is made available under the following conditions:

**Deutsches Urheberrecht**

Weitere Informationen finden Sie unter: / For more information see:

<https://www.uni-augsburg.de/de/organisation/bibliothek/publizieren-zitieren-archivieren/publizieren>



# Mirage phenomena in superconducting quantum corrals

Markus Schmid\* and Arno P. Kampf\*\*

Theoretische Physik III, Elektronische Korrelationen und Magnetismus, Institut für Physik,  
Universität Augsburg, 86135 Augsburg, Germany

*Dedicated to Bernhard Mühlischlegel on the occasion of his 80th birthday*

We investigate the local density of states and the order parameter structure inside an elliptic quantum corral on surfaces of isotropic and anisotropic superconductors. The Bogoliubov-de Gennes equations are solved in the presence of non-magnetic and magnetic impurities. We observe and discuss a variety of mirage and anti-mirage phenomena, which specifically reflect the nature of the superconducting pairing state.

## 1 Introduction

Understanding impurity effects was one of the early, classical tasks for the theory of superconductivity [1,2]. The Anderson theorem explained why non-magnetic impurity scatterers do not destroy conventional, isotropic  $s$ -wave superconductivity [3]. For unconventional superconductors, however, both non-magnetic and magnetic impurities are pairbreaking and the sensitivity to impurities and the concomitant suppression of superconductivity may even serve as a fingerprint of an unconventional pairing state. It took three decades after the development of the BCS theory of superconductivity, before experimental studies of impurity effects on microscopic length scales became possible – mostly due to the advance of scanning tunneling microscopy (STM). The need for experimental probes with a high spatial resolution arose from the discovery of a continuously growing number of unconventional singlet and even triplet superconductors; ruthenates and high-temperature cuprate superconductors belong to the most prominent examples.

During the last decade it has furthermore become possible to manipulate surface structures on the atomic level. In particular the achievements in the research group of D. Eigler led to the design of closed atomic arrangements of adatoms on metallic surfaces [4,5]. In these quantum corrals with circular or elliptical shape electrons are confined to well defined geometries and STM techniques were applied to explore the structure of quantum mechanical wavefunctions and their interference patterns [5,6]. Quantum mirage phenomena are observed, when an additional impurity atom is placed at one focus of an elliptic corral [7]. The terminology of quantum mirages is hereby defined by the observation that mirror images of the local density of states pattern around the impurity at one focus point appear also at the second impurity free focus. In subsequent studies even Kondo resonances could be detected at the impurity-free focus point, if a magnetic impurity adatom was placed in the other focus [8].

---

\* Corresponding author E-mail: markus.schmid@physik.uni-augsburg.de

\*\* E-mail: arno.kampf@physik.uni-augsburg.de

Similar mirage phenomena are expected for elliptic corrals on superconducting surfaces. The local suppression of the superconducting order parameter around an impurity at a selected point in the corral should be transferred to image structures due to standing wave patterns extending over the entire area of the elliptic corral. Superconducting quantum corrals therefore provide unique systems to study the combined effects of impurity induced fingerprint structures of the pairing state and the mirage phenomena of interfering quantum mechanical waves. With the assumption that a superconducting state is established in the bulk and on the surface of the substrate material we discuss in this paper the expected phenomena within the framework of BCS theory and the Bogoliubov-de Gennes equations.

## 2 The model

We consider the following mean-field Hamiltonian for an isotropic and an anisotropic singlet superconductor, respectively, with magnetic or non-magnetic impurities

$$H = \sum_{\sigma} \int d^2\mathbf{r} \psi_{\sigma}^{\dagger}(\mathbf{r}) H_0 \psi_{\sigma}(\mathbf{r}) + H_{s/d} + H_{\text{imp}} \quad (1)$$

with  $H_0 = (-\frac{\hbar^2}{2m} \nabla^2 - \mu) + V(\mathbf{r})$ .  $\mu$  is the chemical potential, and  $V(\mathbf{r})$  is a hard-wall potential, which confines the electrons to the interior of an elliptic corral. The Schrödinger equation for particles in an elliptic geometry was previously solved analytically; the resulting eigenfunctions are a combination of Mathieu functions  $ce_r$ ,  $se_r$  and modified Mathieu functions  $Ce_r$ ,  $Se_r$  [9, 10]:

$$\varphi_{r,n_c}^c(\theta, \eta) = ce_r(\theta, k_n^c) Ce_r(\eta, k_n^c), \quad (2)$$

$$\varphi_{r,n_s}^s(\theta, \eta) = se_r(\theta, k_n^s) Se_r(\eta, k_n^s), \quad (3)$$

where  $\theta$  and  $\eta$  are elliptical coordinates.  $r, n_{c(s)}$  enumerate the quantum numbers for the eigenstates. Their eigenenergies [9]

$$\epsilon = \frac{2\hbar^2}{(ae)^2 m} k_{r,n}^{c/s} \quad (4)$$

are determined by the zeros of the modified Mathieu functions  $k_{r,n}^{c/s}$ .  $a$  denotes the length of the semimajor axis and  $e$  the eccentricity of the ellipse;  $m$  is the electron mass.

For an isotropic  $s$ -wave superconductor with an attractive contact interaction  $H_s$  is given by

$$H_s = - \int d^2\mathbf{r} [\psi_{\uparrow}^{\dagger}(\mathbf{r}) \psi_{\downarrow}^{\dagger}(\mathbf{r}) \Delta(\mathbf{r}) + h.c.], \quad (5)$$

where  $\Delta(\mathbf{r}) = g \langle \psi_{\downarrow}(\mathbf{r}) \psi_{\uparrow}(\mathbf{r}) \rangle$  is the order parameter and  $g > 0$  the pairing interaction strength. Similarly, the mean-field Hamiltonian for a singlet superconductor with a spatially extended pairing interaction is described by

$$H_d = - \int d^2\mathbf{r} \int d^2\mathbf{r}' [\psi_{\uparrow}^{\dagger}(\mathbf{r}) \psi_{\downarrow}^{\dagger}(\mathbf{r}') \Delta(\mathbf{r}, \mathbf{r}') + h.c.], \quad (6)$$

where the order parameter  $\Delta(\mathbf{r}, \mathbf{r}') = g(\mathbf{r}, \mathbf{r}') \langle \psi_{\downarrow}(\mathbf{r}') \psi_{\uparrow}(\mathbf{r}) \rangle$  depends on both coordinates  $\mathbf{r}$  and  $\mathbf{r}'$  of the electrons forming the Cooper pair. Our ansatz for the pairing interaction is  $g(\mathbf{r}, \mathbf{r}') = g \delta(|\mathbf{r} - \mathbf{r}'| - R)$  and assumes an attraction for electrons at a distance  $R$ ; this lengthscale  $R$  should be set by the size of a typical crystal lattice constant. Although  $g(\mathbf{r}, \mathbf{r}')$  is an isotropic real space interaction, it gives rise to an anisotropic local order parameter as we discuss below. The impurity potentials for magnetic (−) and non-magnetic (+) impurities are described by

$$H_{\text{imp}} = \int d^2\mathbf{r} U(\mathbf{r}) [\psi_{\uparrow}^{\dagger}(\mathbf{r}) \psi_{\uparrow}(\mathbf{r}) \pm \psi_{\downarrow}^{\dagger}(\mathbf{r}) \psi_{\downarrow}(\mathbf{r})], \quad (7)$$

where  $U(\mathbf{r}) = \sum_i^n U_0 \delta(\mathbf{r} - \mathbf{r}_i)$  with impurity positions  $\mathbf{r}_i$ . In this model for the magnetic scattering center the impurity spins are treated as classical spins,  $S \gg 1$  [11, 12], which is a reasonable assumption e.g. for Mn and Gd adatom impurities on a niobium surface [13].

The mean-field Hamiltonian Eq. (1) is diagonalized by the transformation

$$\psi_\sigma(\mathbf{r}) = \sum_n [u_n(\mathbf{r})\alpha_{n\sigma} + \text{sgn}(\sigma)v_n(\mathbf{r})\alpha_{n-\sigma}^\dagger], \quad (8)$$

$$\alpha_{n\sigma} = \int d^2\mathbf{r} [u_n(\mathbf{r})\psi_\sigma(\mathbf{r}) - \text{sgn}(\sigma)v_n(\mathbf{r})\psi_{-\sigma}^\dagger(\mathbf{r})], \quad (9)$$

where  $\alpha_{n\sigma}$  describes a superconducting quasiparticle with spin  $\sigma$  and energy  $E_n$ . The ansatz (8) leads to the Bogoliubov-de Gennes equations

$$[H_0 + U(\mathbf{r})]u_n(\mathbf{r}) + \int d^2\mathbf{r}' \Delta(\mathbf{r}, \mathbf{r}')v_n(\mathbf{r}') = E_n u_n(\mathbf{r}), \quad (10)$$

$$\int d^2\mathbf{r}' \Delta(\mathbf{r}, \mathbf{r}')u_n(\mathbf{r}') - [H_0 \pm U(\mathbf{r})]v_n(\mathbf{r}) = E_n v_n(\mathbf{r}), \quad (11)$$

where the  $+/-$  sign in Eq. (11) corresponds to non-magnetic/magnetic impurities, respectively. These equations are simplified in the case of an isotropic superconductor, where the pairing-interaction is pointlike, and therefore  $\Delta(\mathbf{r}, \mathbf{r}') = \delta(\mathbf{r} - \mathbf{r}') \Delta(\mathbf{r})$ . The order parameter  $\Delta(\mathbf{r})$  is determined self-consistently from the condition

$$\Delta(\mathbf{r}) = g \sum_n u_n(\mathbf{r})v_n(\mathbf{r}) [1 - 2f(E_n)], \quad (12)$$

where  $f(E)$  denotes the Fermi function. For an anisotropic superconductor with a finite range pairing interaction we have instead

$$\Delta(\mathbf{r}, \mathbf{r}') = g(\mathbf{r}, \mathbf{r}') \sum_n \{u_n(\mathbf{r})v_n(\mathbf{r}') [1 - f(E_n)] - u_n(\mathbf{r}')v_n(\mathbf{r}) f(E_n)\}. \quad (13)$$

In order to solve the Bogoliubov-de Gennes equations (10) and (11) we expand  $u_n(\mathbf{r})$  and  $v_n(\mathbf{r})$  in terms of free electron eigenfunctions inside the elliptic corral [9]

$$u_n(\mathbf{r}) = \sum_k u_{kn} \varphi_k(\mathbf{r}), \quad (14)$$

$$v_n(\mathbf{r}) = \sum_k v_{kn} \varphi_k(\mathbf{r}), \quad (15)$$

where  $k$  enumerates all the eigenstates given in Eqs. (2) and (3). For the ground-state energies of the isotropic (Eq. (16)) and the anisotropic (Eq. (17)) superconductor we find

$$E_g^s = 2 \sum_n \int d^2\mathbf{r} [v_n(\mathbf{r})H_0v_n(\mathbf{r}) - \Delta(\mathbf{r})u_n(\mathbf{r})v_n(\mathbf{r})], \quad (16)$$

$$E_g^d = \sum_n \int d^2\mathbf{r} \left[ 2v_n(\mathbf{r})H_0v_n(\mathbf{r}) - \int d^2\mathbf{r}' \Delta(\mathbf{r}, \mathbf{r}') (u_n(\mathbf{r})v_n(\mathbf{r}') + u_n(\mathbf{r}')v_n(\mathbf{r})) \right]. \quad (17)$$

The local density of states (LDOS) is obtained from

$$N(\mathbf{r}, \omega) = \sum_n [u_n^2(\mathbf{r})\delta(\omega - E_n) + v_n^2(\mathbf{r})\delta(\omega + E_n)], \quad (18)$$

and the total density of states (DOS) is  $N(\omega) = \int d^2\mathbf{r} N(\mathbf{r}, \omega)$ .

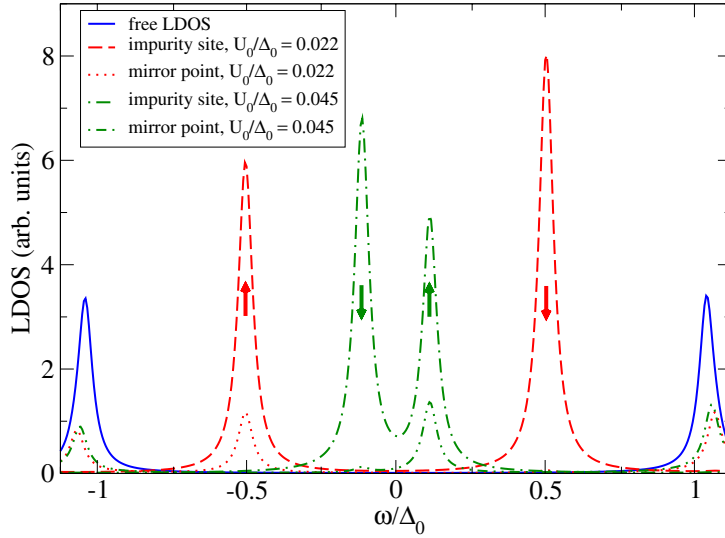


**Fig. 1** Local density of states (LDOS) for an isotropic superconductor with a magnetic impurity at the right focus. Dashed and dash-dotted lines show the LDOS at the impurity site ( $0.5a, 0$ ), dotted and dash-double-dotted lines show the LDOS at the mirror point ( $-0.5a, 0$ ). The arrows ascribe the spin projection to the particle and the hole component of the bound state.

### 3 Results

For the elliptic corral we choose its eccentricity  $e = 0.5$  and the length of the semi-major axis  $a = 150 \text{ \AA}$ ; these two parameters determine the single-particle eigenenergies and -states. With an approximate electronic density of one electron per  $6 \text{ \AA} \times 6 \text{ \AA}$  square the total number of electrons in the corral is  $N = 1726$ . With this choice the  $863^{\text{rd}}$  eigenstate at the Fermi energy  $\epsilon_F$  has a large probability density at the foci, which is a favorable situation for the occurrence of mirage phenomena. For an isotropic superconductor the mirage phenomenon is observed, whenever there is one of these non-zero probability density eigenstates lying inside the energy gap. For our choice of the pairing interaction strength  $g = 1.0 \times 10^{-3} \epsilon_F$  the energy gap  $\Delta_0$  stretches over about 50 eigenstate energies, where several of these states have the required property. Hence, the existence of mirage phenomena for an isotropic superconducting surface does not depend sensitively on the position of the Fermi energy, in contrast to a metallic, normal conducting surface [9] and also in contrast to an anisotropic superconductor, as we discuss below.

#### 3.1 Isotropic $s$ -wave superconductor

We start our analysis with a corral on the surface of an isotropic  $s$ -wave superconductor. In the presence of non-magnetic impurities the system remains time-reversal invariant. These impurities do not break Cooper pairs, which are built from Kramers-degenerate electronic states [3]. Consequently, no additional states are created in the renormalized energy gap. Magnetic impurities on the contrary, are pair-breaking defects, because the spin-up electron of the Cooper pair is repelled ( $U_0 > 0$ ) and the spin-down electron is attracted by the impurity, leading to a quasiparticle bound state with a spin-down particle peak and a spin-up hole peak in the LDOS shown in Fig. 1 (dashed and dotted curves), where the impurity is located at the right focus of the ellipse. The LDOS at the impurity site vanishes at the gap edge energies, while the LDOS at the mirror point (dotted line) is finite at these energies. The total spectral weight of both peaks, i.e. the spatially and energy (between the gap edge energies  $-\Delta_0$  and  $\Delta_0$ ) integrated LDOS is unity, characterizing one localized quasiparticle. Hence, the bound state corresponding to the dashed line is a local spin-down quasiparticle state (see also Fig. 2, unfilled triangles), where the spin projection of the particle component is antiparallel and that of the hole component is parallel to the impurity spin. This is the same phenomenon known for the extended  $s$ -wave superconductor without confining boundaries [12]. The dash-dotted and dash-double-dotted curves in Fig. 1 show the LDOS for a stronger impurity potential. The difference now is that the spins of the particle and the hole peak have changed, i.e. we find a spin-up quasiparticle (compare

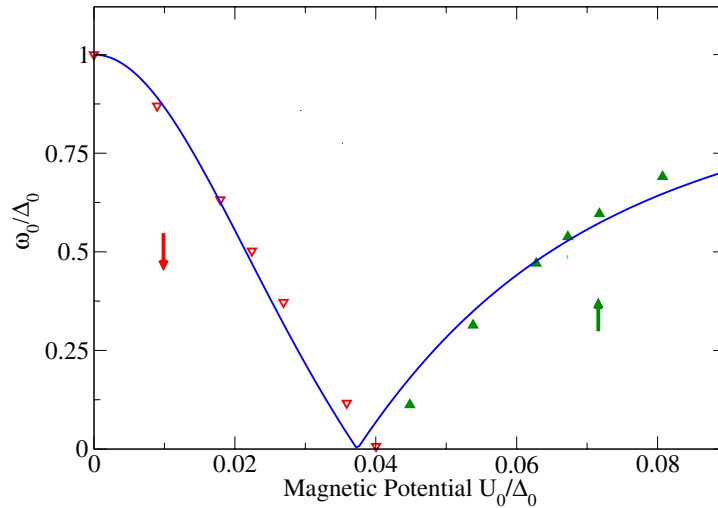


**Fig. 2** Bound-state energy for an elliptic quantum corral (triangles) with a magnetic impurity at the right focus  $(0.5a, 0)$  compared with the bound-state energy for a magnetic impurity on an open surface of a  $s$ -wave superconductor (solid curve); the arrows mark the spin-direction of the particle component of the quasiparticle bound state. Filled/unfilled triangles correspond to a spin-down/spin-up quasiparticle, respectively;  $U_0/\epsilon_F \cong 0.03U_0/\Delta_0$ .

with Fig. 2, filled triangles). This change is due to the fact that both peaks cross the Fermi energy at a critical impurity potential strength  $U_c$ .

In the corral geometry we observe the two-peak structure in the LDOS not only at the impurity site e.g. at one focus point, but also – with some attenuation – at the impurity free focus (dotted and dash-double-dotted lines) [14]. The mirage effect is only strong at one of the two peaks at the mirror point LDOS. There the particle peak carries very little spectral weight for  $U_0 < U_c$  (see Fig. 1, dotted line), and so does the hole peak for  $U_0 > U_c$ . But with increasing  $U_0$  the particle and hole peaks at the mirror point are both growing. We emphasize that the LDOS peaks at the mirror point are at the same resonance energies as in the LDOS at the impurity site, because they belong to the same bound state with energy  $\omega_0$ . This is the quantum mirage effect in the LDOS for an elliptic corral built on the surface of an isotropic  $s$ -wave superconductor. As expected, we find this effect to be very robust against a change in the Fermi energy and thus the electron density. Moreover this mirage effect remains almost unaffected by an additional perturbation in form of a second magnetic impurity placed anywhere else inside the corral.

Since the bound-state peaks at energies  $\omega = \pm\omega_0$ , split off from the gap edges, they move with increasing potential strength  $U_0$  symmetrically towards the Fermi energy (see Fig. 2).  $\omega_0$  therefore decreases until it reaches the chemical potential for a critical potential  $U_c$ , which depends on the impurity position  $\mathbf{r}_0$ . At  $U_0 = U_c$  the bound state becomes a zero energy state, and the ground state of the superconductor becomes unstable. The existence of this critical point, which signals a ground-state level crossing transition, was first pointed out by Sakurai for  $s$ -wave superconductors with magnetic impurities [15]. At  $U_c$  the system undergoes a first order phase transition from a spin zero to a spin  $-\frac{1}{2}$  ground state [12, 15]. While the condensate ground state for  $U_0 < U_c$  consists only of Cooper pairs, the new ground state for  $U_0 > U_c$  contains an additional spin-down electron (or up-spin hole). The impurity induced bound state is now a spin-up quasiparticle (Fig. 1, dash-dotted and dash-double-dotted curves and Fig. 2, filled triangles). A further increase of  $U_0$  in this regime ( $U_0 > U_c$ ) is accompanied by a spatial shift of the LDOS at the resonance energies away from the impurity position. This spatial redistribution of the spectral weight leads to decreasing heights of the bound-state peaks in the LDOS Fig. 1 at the impurity position (right focus) and an accompanying increase of the peak heights at the impurity free focus. Note that the total spectral weight of the bound-state peaks always remains unity. Hence we observe a transition from a mirage-effect for small  $U_0$  to an anti-mirage-effect for large  $U_0$ .

We compare our self-consistent solutions of the Bogoliubov-de Gennes equation for a corral with the results for an open surface using the following formula for the bound-state energies [12]

$$\omega_0 = \Delta_0 \frac{|1 - (\pi N_F)^2 U_0^2|}{1 + (\pi N_F)^2 U_0^2}, \quad (19)$$

where  $N_F$  is the normal state DOS at the Fermi energy. Eq. (19) is obtained from the non-self-consistent T-matrix formalism, which proved to be sufficient and even quantitatively accurate for the description of magnetic impurity induced bound states in  $s$ -wave superconductors without confining walls [12]. In Fig. (2) we use Eq. (19) with  $\pi N_F \rightarrow \overline{N_F}$  (solid curve), where  $\overline{N_F}$  describes the mean density of states averaged over an energy window  $\epsilon_F \pm \Delta_0$  in the normal state. Fig. 2 shows that the bound-state energies in the elliptic corral are well described by Eq. (19). Comparing the self-consistent and non-self-consistent results for our corral, we find indeed only small differences: neither the quasiparticle energies are shifted notably nor the heights of the quasiparticle peaks are modified significantly.

Another interesting quantity is the renormalized local order parameter  $\Delta(\mathbf{r})$  given by Eq. (12). We observe a suppression of  $\Delta(\mathbf{r})$  at the impurity site, where the lengthscale of the suppression and the wavelength of the order parameter oscillations is given approximately by the Fermi wavelength  $\lambda_F = 2\pi\hbar/\sqrt{2m\epsilon_F} \approx 15\text{\AA}$ , but seems to be independent of the size of the energy gap  $\Delta_0$ . Remarkably, the local order parameter at the impurity position changes discontinuously from a positive to a negative value, when  $U_0$  crosses the critical potential strength  $U_c$  [12, 17]. For a non-magnetic impurity the reduction of  $\Delta(\mathbf{r})$  in the vicinity of the impurity is due to the repulsive potential for both spin directions resulting in a reduced electronic density at and near the impurity site and therefore to a reduced local pairing amplitude. In Fig. 3 a magnetic impurity is placed at the right focus point. All one-particle eigenstates with a large probability density at the right focus have a large probability density at the left focus as well. The difference plot of the order parameter Fig. 3 strongly resembles the 863<sup>rd</sup> eigenstate, implying that  $\Delta(\mathbf{r})$  is suppressed not only at the impurity site (right focus), but almost symmetrically at the impurity free (left) focus, which we therefore call an order parameter mirage effect. We note that the order parameter is negative at the impurity site in Fig. 3.

If there are magnetic impurity spins in both foci, their antiparallel alignment leads to a lower ground-state energy Eq. (16). Moreover we observe that the order parameter suppression is about six times stronger for a parallel than for an antiparallel impurity spin alignment. A parallel alignment leads to a four-peak structure in the LDOS, because there are two similar states localized at each impurity, which are hybridizing and therefore splitting into bonding and antibonding states [14, 16]. If the impurity spins are aligned antiparallel,

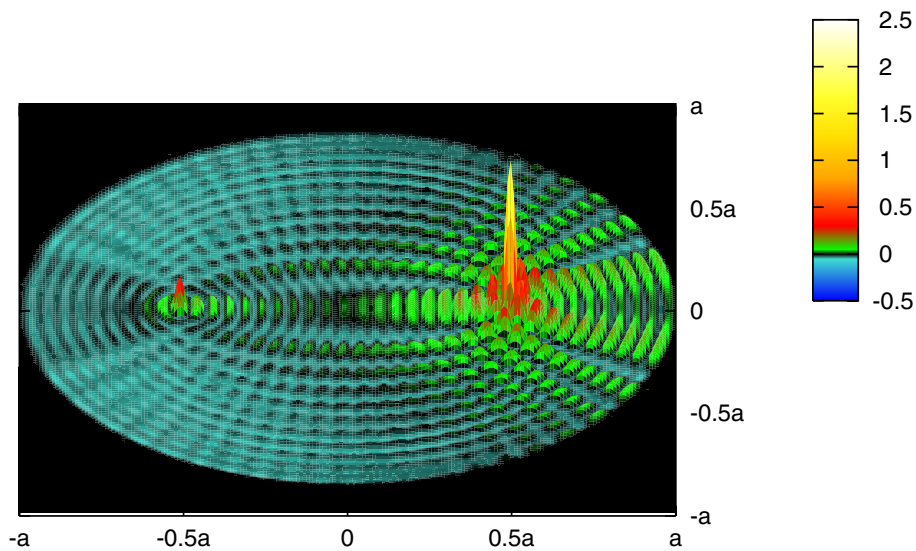


**Fig. 3** Difference plot of the local order parameter  $\frac{\Delta^0(\mathbf{r}) - \Delta^i(\mathbf{r})}{\Delta_0}$  in the elliptic corral;  $\Delta^i(\Delta^0)$  is the order parameter in the presence (absence) of the impurity; the magnetic impurity is at the right focus  $(0.5a, 0)$ ,  $U_0/\Delta_0 = 0.135$ .

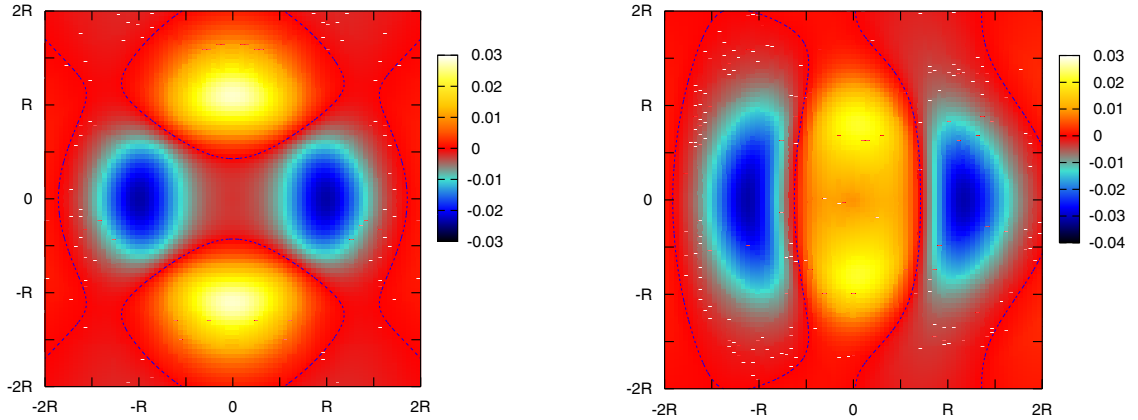


**Fig. 4** Local order parameter  $\Delta(\mathbf{r}, \mathbf{r} + \mathbf{r}')$  in units of  $\epsilon_F$  for the anisotropic superconductor for a fixed  $\mathbf{r}$  plotted as a function of  $\mathbf{r}' = (x', y')$  with  $x', y' \in [-2R, 2R]$ ; the dashed lines mark the order parameter nodes;  $\mathbf{r} = (0, 0)$  in the left panel and  $\mathbf{r} = (0.44a, 0)$  in the right panel.

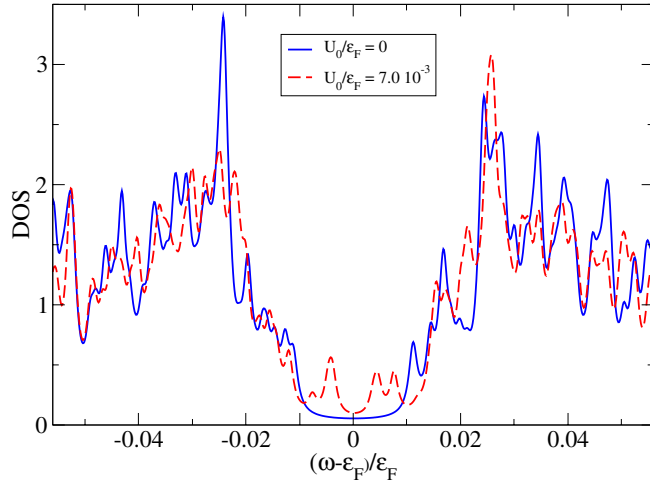


**Fig. 5** Density of states (DOS) for the anisotropic superconductor with a non-magnetic impurity at  $(0.44a, 0)$ .

we find only two peaks inside the energy gap. The intensity of the hybridization depends in general on the distance between the two impurities; for a corral geometry this dependence is quite complex.

### 3.2 Anisotropic superconductor

Now we assume the pairing interaction  $g(\mathbf{r}, \mathbf{r}')$  to be attractive in a distance of a typical crystal lattice constant  $R \cong 0.04a = 6\text{\AA}$ . In this case the order parameter  $\Delta(\mathbf{r}, \mathbf{r}')$  depends on the position inside the corral as well as on the relative coordinate. Although the interaction is still isotropic, the order parameter is now anisotropic. In Fig. 4 (left panel) we show the order parameter in the center of the ellipse, where we identify a  $d$ -wave like structure with sign changes and nodes at angles near  $45^\circ$  with respect to the semimajor axis. At the center the order parameter is least affected by the confining corral, but except for this point of highest symmetry, the structure of the local order parameter is distorted in a complex way. An example for a remarkably complicated symmetry and local structure of  $\Delta(\mathbf{r}, \mathbf{r}')$  is shown in the right panel of Fig. 4. The spatially extended pairing interaction leads to a V-shape-resembling DOS (see Fig. 5, solid curve), with no sharp gap edges. Furthermore, the DOS has no particle-hole symmetry, because of the asymmetric distribution of eigenenergies for the corral eigenfunctions.

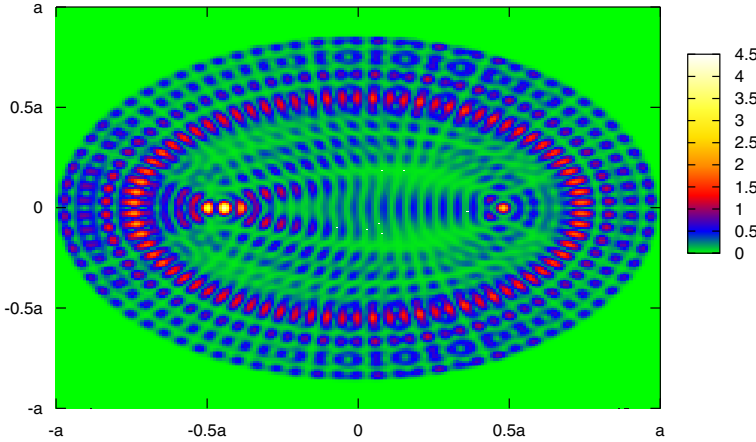


**Fig. 6** Local density of states (LDOS) for the anisotropic superconductor with a non-magnetic impurity at  $(0.44a, 0)$ ;  $U_0/\epsilon_F = 7.0 \times 10^{-3}$ . The LDOS is shown at the positive resonance energy  $\omega_L^+ = 2.8 \times 10^{-3} \epsilon_F$  (see text).

While non-magnetic impurities do not give rise to localized states in a  $s$ -wave superconductor, they do have a pair-breaking effect in an anisotropic superconductor [18]. For a non-magnetic impurity placed at different positions inside the corral we calculate the local order parameter, the DOS, and the LDOS. In the DOS we always find bound-state peaks, which move towards the Fermi energy as  $U_0$  increases, but never reach  $\epsilon_F$ . Hence, we do not observe a zero-energy-peak in agreement with the results for an open surface in a particle-hole asymmetric situation [12, 19]. The DOS is modified over the entire energy range as shown in Fig. 5. For weak impurity potentials we observe a two-peak structure in the DOS near the Fermi energy, but after exceeding some critical potential  $\tilde{U}_c$ , which depends again on the impurity position  $\mathbf{r}_0$ , each of the two peaks starts to split into two, so that a four-peak structure emerges near  $\omega = \epsilon_F$  (see Fig. 5). At the resonance energies for small  $U_0$  (two-peak regime) we find, that the bound state has a large LDOS in the vicinity of the impurity. By increasing  $U_0$  the original bound state acquires admixtures of the 862<sup>nd</sup> and 866<sup>th</sup> state [20]. Above the critical potential  $\tilde{U}_c$ , we identify the 866<sup>th</sup> state either at both outer or both inner peaks of the four-peak low-energy DOS, while the LDOS at the two other peaks consists of the small  $U_0$  bound state mixed with a contribution of the 862<sup>nd</sup> state. Hence the splitting of the bound state energy corresponds to a "demixing" of the contributing states, which form the bound state. We observed this behavior at different impurity positions on the semimajor axis, but the occurrence of a four-peak structure nevertheless depends sensitively on the Fermi energy. Slight variations of the electronic densities can lead to two-peak structures in the DOS, irrespective of the impurity potential strength.

In order to show a few of a large variety of interesting and astonishing effects we calculate the LDOS in the presence of a non-magnetic impurity in particular at the right focus  $(0.5a, 0)$ , at  $(0.44a, 0)$ , and at the center  $(0,0)$ . Interestingly, the important states (862<sup>nd</sup> and 866<sup>th</sup>) mentioned above are the only contributions to the bound state for an impurity in a focus point. These states have a zero LDOS on the entire semimajor axis, but several maxima about a lattice constant away from the focus. This bound state shows an almost perfect reflection symmetry with respect to the semiminor axis. Shifting the impurity a distance  $1.5R$  away from the right focus to  $(0.44a, 0)$ , we observe that the LDOS at the lower resonance energies  $\omega_L^\pm = \pm 2.8 \times 10^{-3} \epsilon_F$  has a strong contribution of the 863<sup>rd</sup> state and, as discussed before, a weaker contribution of the 862<sup>nd</sup> state. Fig. 6 shows the LDOS at the positive resonance energy  $\omega_L^+$ . While the LDOS at the impurity site itself is zero, we observe a maximum in the LDOS at the mirror point. The impurity induces asymmetrically spectral weight around both foci, whereas the height is larger at the left than at the right focus, which is close to the impurity. Thus, we observe a surprising, strong anti-mirage effect in the LDOS at all resonance energies with a non-magnetic impurity at  $(0.44a, 0)$  independent of the potential strength  $U_0$ .

In Fig. 7 we show the LDOS with an impurity located at the center of the ellipse at the energy of the higher positive resonance energy  $\omega_H^+ = 7.6 \times 10^{-3} \epsilon_F$ . We identify the 862<sup>nd</sup> eigenstate again, which determines the region near the boundary of the ellipse and consists of rings of peaks aligned along four ellipses. The

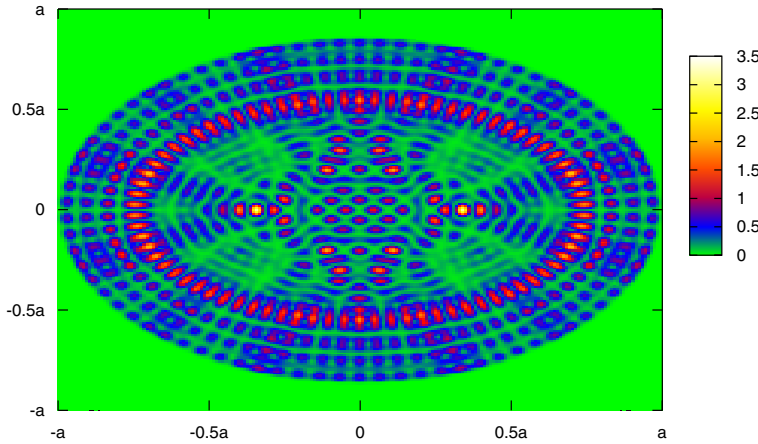


**Fig. 7** Local density of states (LDOS) with a non-magnetic impurity at the center  $(0,0)$  of the ellipse;  $U_0/\epsilon_F = 14.0 \times 10^{-3}$ . The LDOS is shown at the resonance energy  $\omega_H^+ = 7.6 \times 10^{-3} \epsilon_F$  (see text).

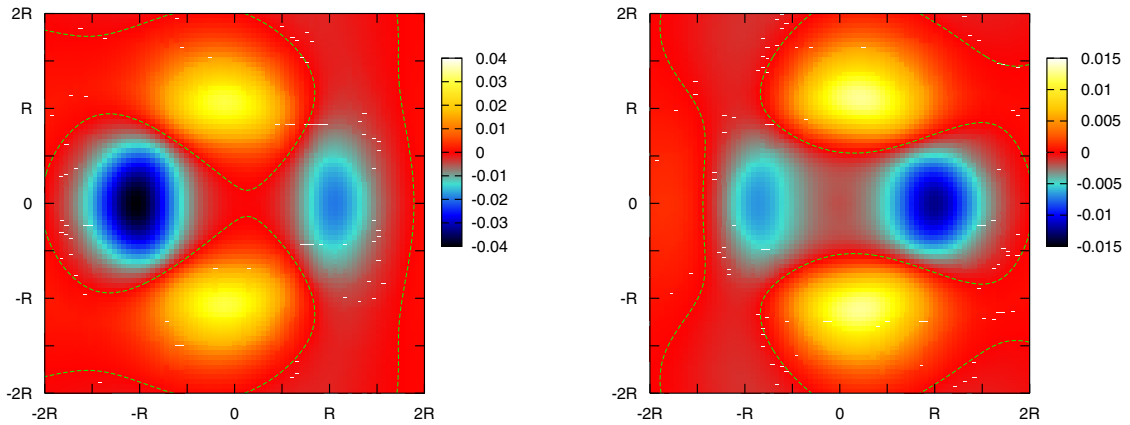


**Fig. 8** Local order parameter  $\Delta(\mathbf{r}, \mathbf{r} + \mathbf{r}')$  for a fixed  $\mathbf{r}$  with a non-magnetic impurity at  $(0.44a, 0)$ ;  $U_0/\epsilon_F = 2.8 \times 10^{-3}$ ;  $\mathbf{r} = (-0.44a, 0)$  in the left panel and  $\mathbf{r} = (0.44a, 0)$  in the right panel. See also the caption of Fig. 4.

structure of the LDOS in the vicinity of the impurity is in fact more influenced by the symmetry of the local order parameter than the geometry of the problem. For example, in a range of a few lattice constants around the center there is no LDOS along the diagonal directions, and locally there is almost a fourfold symmetry as for the absolute value of the order parameter in Fig. 4 (left panel) [21].

In the vicinity of the impurity site the order parameter is reduced strongly by a non-magnetic impurity. This becomes obvious by comparing the right panels of Figs. 4 and 8, where the impurity is located at  $(0.44a, 0)$ . Moreover we observe here and quite generally a modification of the spatial structure and the symmetry of the local order parameter, which depends sensitively on the potential strength  $U_0$ . Interestingly the new, impurity induced spatial structure resembles more a  $d$ -wave-like symmetry than the original structure. Fig. 8 clearly indicates, that this  $d$ -wave-like order parameter structure is projected to the impurity free mirror point. Instead of a reduction, the order parameter is actually enhanced at the mirror point. As in the LDOS we therefore also observe an anti-mirage effect for the order parameter. The order parameter at  $(0.44a, 0)$  is changed to a structure similar as in Fig. 8 (right panel), if an impurity is located at the center (!) of the ellipse. In general we find, that the magnitude of the order parameter is not only reduced over the entire area of the corral, but also modified with respect to its local spatial symmetry.

Regarding the connection between the spatial structure of the LDOS in the vicinity of the impurity and the order parameter, we encounter three different situations. (i) the LDOS resembles the order parameter in the absence of an impurity, (ii) the LDOS resembles the order parameter in the presence of an impurity,

and (iii) there is no connection at all between the two. The latter is observed for example for a focus point impurity. We find the behavior (i) only for an impurity at the center of the corral, for large impurity potentials, and at positive resonance energies. For smaller impurity potentials we are back to case (ii), where again the LDOS shows the structure of the order parameter with an impurity only at positive resonance energies. This second case seems to reflect the more generic situation. Hence, the LDOS in the presence of a non-magnetic impurity inside the corral can directly reveal the structure and the local symmetry of the order parameter.

## 4 Conclusion

We have observed a rich variety of mirage- and anti-mirage-phenomena not only in the LDOS, but also for the local order parameter structure. The induced patterns in both quantities in the vicinity of an impurity lead to mirror images in impurity-free regions, which are characteristic for both, the structure of the electronic wavefunctions in the elliptic geometry and the nature of the superconducting state. With the continuing advances of STM techniques and the already achieved capabilities for the design of atomic corral arrangements on metallic surfaces the realization of quantum corrals on superconducting surfaces indeed appears to be possible. From our model analysis we are led to expect intriguingly rich structures in the LDOS patterns, which by themselves contain information about the nature of the superconducting state.

**Acknowledgements** One of the authors (APK) wishes to express his special gratitude for the guidance and support during and ever after his doctoral thesis work supervised by Bernhard Mühlischlegel. This work was supported by the Deutsche Forschungsgemeinschaft through SFB 484.

## References

- [1] A.A. Abrikosov, L.P. Gorkov, and I.E. Dzyaloshinski, *Methods of Quantum Field Theory in Statistical Physics* (Dover Publications, Inc., New York, 1963).
- [2] J.R. Schrieffer, *The Theory of Superconductivity* (Benjamin Press, New York, 1964).
- [3] P.W. Anderson, *Phys. Rev. Lett.* **3**, 325 (1959).
- [4] M.F. Crommie, C.P. Lutz, and D.M. Eigler, *Nature (London)* **363**, 524 (1993); *Science* **262**, 218 (1993).
- [5] E.J. Heller, M.F. Crommie, C.P. Lutz, and D.M. Eigler, *Nature (London)* **369**, 464 (1994).
- [6] J. Kliewer, R. Berndt, E.V. Chulkov, V.M. Silkin, P.M. Echenique, and S. Crampin, *Science* **288**, 1899 (2000).
- [7] H.C. Manoharan, C.P. Lutz, and D.M. Eigler, *Nature (London)* **403**, 512 (2000).
- [8] For reviews of mirage effects in quantum corrals see: G.A. Fiete and E.J. Heller, *Rev. Mod. Phys.* **75**, 933 (2003); A.A. Aligia and A.M. Lobos, *J. Phys.: Cond. Mat.* **17**, S1095 (2005).
- [9] M. Schmid and A. Kampf, *Ann. Phys. (Leipzig)* **12**, 463 (2003).
- [10] D. Porras, J. Fernández-Rossier, and C. Tejedor, *Phys. Rev. B* **63**, 155406 (2001).
- [11] H. Shiba, *Prog. Theo. Phys.* **40**, 435 (1968).
- [12] M.I. Salkola, A.V. Balatsky, and J.R. Schrieffer, *Phys. Rev. B* **55**, 12648 (1997).
- [13] A. Yazdani, B.A. Jones, C.P. Lutz, M.F. Crommie, and D.M. Eigler, *Science* **275**, 1767 (1997).
- [14] D.K. Morr and N.A. Stavropoulos, *Phys. Rev. Lett.* **92**, 107006 (2004).
- [15] A. Sakurai, *Progr. Theor. Phys.* **44**, 1472 (1970).
- [16] M.E. Flatté and D.E. Reynolds, *Phys. Rev. B* **61**, 14810 (2000).
- [17] M.E. Flatté and J.M. Byers, *Phys. Rev. B* **56**, 11213 (1997).
- [18] L.P. Gorkov, *Pis'ma Zh. Eksp. Teor. Fiz.* **40**, 351 (1984).
- [19] J. Zhu, T.K. Lee, C.S. Ting, and C. Hu, *Phys. Rev. B* **61**, 8667 (2000).
- [20] We note that the bound states can be expanded in terms of the corral eigenfunctions  $\varphi_k(\mathbf{r})$ . Often we observe that only one or two of these states with energies near  $\epsilon_F$  contribute significantly in the expansion of the bound state.
- [21] For an extended, unbounded system similar observations were reported in: S. Haas and K. Maki, *Phys. Rev. Lett.* **85**, 2172 (2000).